

Use of 3D Printed Bone Plate in Novel Technique to Surgically Correct Hallux Valgus Deformities

Kathryn E. Smith, PhD,* Kenneth M. Dupont, PhD,* David L. Safranski, PhD,*
Jeremy W. Blair, MBA, BSME,* Dawn R. Buratti, DPM,† Vladimir Zeetser, DPM,†
Ryan Callahan, DO,‡ Jason S. Lin, MD,‡§ and Ken Gall, PhD*||

Summary: Three-dimensional (3D) printing offers many potential advantages in designing and manufacturing plating systems for foot and ankle procedures that involve small, geometrically complex bony anatomy. Here, we describe the design and clinical use of a Ti-6Al-4V extra low interstitial bone plate (FastForward Bone Tether Plate; MedShape, Inc., Atlanta, GA) manufactured through 3D printing processes. The plate protects the second metatarsal when tethering suture tape between the first and second metatarsals and is a part of a new procedure that corrects hallux valgus (bunion) deformities without relying on doing an osteotomy or fusion procedure. The surgical technique and 2 clinical cases describing the use of this procedure with the 3D printed bone plate are presented within.

Key Words: 3D printing—fastforward—bone plate—bone tether plate—titanium—hallux valgus—bunion—metatarsus primus adductus varus.

(Tech Orthop 2016;00: 000–000)

INTRODUCTION: HALLUX VALGUS SURGERY

Over 300,000 hallux valgus correction procedures are performed annually in the United States. The goal of corrective surgery is to restore foot mechanics (alignment, motion, and load distribution) and provide pain relief so that patients can return to their desired activity level. Surgical correction of hallux valgus, or bunion, deformities has been a longstanding challenge for more than a century, with the first case reported in 1870 by Carl Hueter.¹ Over 130 techniques have been described for the treatment of hallux valgus, ranging from bunionelectomies, soft tissue procedures, single or combined osteotomies, and arthrodesis of the first tarsometatarsal or metatarsophalangeal (MTP) joint.^{1–3} This myriad of options suggests that there is no universally accepted optimal solution for hallux valgus. In fact, the lack of consensus continues to promote surgical innovation, particularly in the fields of materials science and mechanical engineering. Modern techniques involving tethering a suture button or suture cerclage,

offer less invasive bone and joint sparing correction approaches, but these procedures place large stresses on the second metatarsal and consequently have introduced additional complications such as second metatarsal fracture.^{4–6} Here, we describe the design and use of a three-dimensional (3D) printed titanium (Ti) alloy [Ti-6Al-4V extra low interstitial (ELI)] plate that is placed on the second metatarsal and addresses the challenges with current joint sparing approaches. The plate is part of the FastForward bunion correction system (MedShape Inc. Atlanta, GA—Fig. 1), which uses robust suture tape fixation to anatomically reduce the intermetatarsal angle (IMA) while shielding the second metatarsal from extreme stresses. This unique approach enables the correction of a wide range of bunion deformities without relying on nonanatomic osteotomies or fusion procedures.

3D PRINTING FOR FOOT AND ANKLE PLATING

Limitations of Traditional Plate Manufacturing Methods

To date, plating for foot and ankle applications has proven challenging given the complex, 3D anatomy of many of the small bones. Many standard plates do not conform to the irregular bony surfaces, cause stress shielding and may result

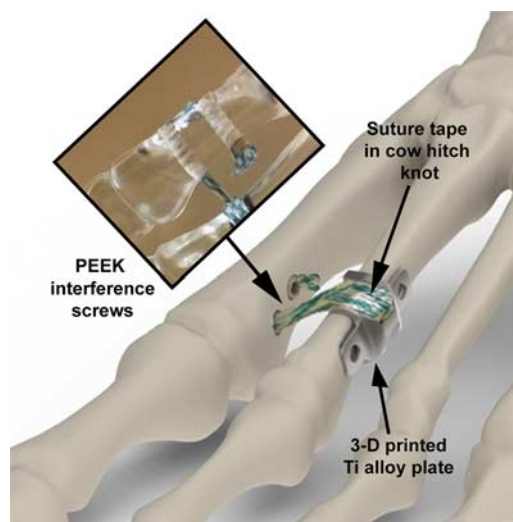


FIGURE 1. Diagram showing the components of the FastForward procedure. The three-dimensional (3D) printed plate rests on the lateral side of the second metatarsal and retains the suture tape around the bone while shielding it from tape friction and tension. Two PEEK interference screws are used to fixate the tape in the first metatarsal (inset image).

From the *MedShape Inc., Atlanta, GA; †Private Practice, Encino, CA; §Samaritan Orthopaedics and Sports Medicine Center; ‡Good Samaritan Regional Medical Center, Corvallis, OR; and ||Department of Mechanical Engineering and Materials Science, Duke University, Durham, NC.

Supported by NIH Small Business Innovation Research Program Grant, National Institute of Arthritis and Musculoskeletal and Skin Diseases, Number 1R43AR068864-01.

K.E.S., K.M.D., D.L.S., and J.B. are employees of and own stock/stock options in MedShape Inc. D.B. and V.Z. are inventors of the FastForward system and receive royalties from MedShape Inc. J.L. and K.G. are consultants of MedShape Inc. and own stock/stock options in MedShape Inc. R.C. declares that he has nothing to disclose.

Address correspondence and reprint requests to Ken Gall, PhD, Department of Mechanical Engineering and Materials Science, Duke University, P.O. Box 90300 Hudson Hall, Durham, NC 27708. E-mail: ken.gall@duke.edu. Copyright © 2016 Wolters Kluwer Health, Inc. All rights reserved.

in patient discomfort due to their relatively thick profile. Plating systems that match the native anatomy have shown to provide more support and stability, potentially allowing patients to return to weight-bearing and regular activity sooner.⁷ The second metatarsal in particular presents its own set of anatomic challenges for plating given its small cross-sectional area and asymmetric geometry. The bone is also mechanically weaker due to its thin cortices and low-density cancellous bone, and thus susceptible to stress fractures.⁵ To provide a mechanically stable construct, a plate must lie in direct apposition to the bone surfaces. Any significant gapping between the bone and the plate can decrease the plate's stability and create large stress concentrations on the bone.⁸⁻¹² For example with joint-sparing bunion correction procedures, the second metatarsal is subjected to bending forces imparted by reducing the first intermetatarsal space with suture material. In this instance, it is important that the force be evenly distributed across the bone to prevent any stress fractures from occurring. Lastly because there is minimal soft tissue surrounding the bones in the foot, plates must be thin or low-profile so as not to protrude or cause any skin irritation.⁸ The absence of bulging underneath the skin is also an aesthetic advantage for patients.¹³

Fabricating plates to closely match the native anatomy of small bones, such as the second metatarsal, can be difficult with conventional methods such as casting or computer numerical control machining.^{14,15} The implant design is often limited by the capabilities of the manufacturing process, particularly when the part has very small geometric features. The cost to fabricate plates using traditional methods will generally increase with increasing part complexity,¹⁶ as expensive molds and tooling are often required.¹⁴ In addition, commonly used plate materials, such as Ti and Ti-6Al-4V alloy, are easily oxidized at high temperature and react with investment casting materials, which can lead to rough surfaces and internal defects.^{15,17,18} Finally, casting shrinkage is a common problem which can reduce the dimensional accuracy of the part, which is essential for small, complex plate architectures.¹⁵

Advantages of 3D Printing

Given the challenges with conventional manufacturing approaches, additive manufacturing, or 3D printing, serves as a cost-effective option for producing small bone plating systems that have unique anatomic, structural, and mechanical requirements.^{19,20} A primary advantage of 3D printing is the ability to produce parts quickly at lower costs compared with traditional manufacturing practices with costs scaling only with the volume of parts fabricated.¹⁶ In addition, 3D printing allows for the inclusion of pores, cutouts, or internal channels, which may be beneficial for providing implant functionality not available in traditionally machined implants. For example, plates manufactured out of Ti alloy often cause stress shielding of the attached bones due to the higher stiffness of the Ti alloy as compared with the stiffness of bone.²¹ Incorporation of pores or thinning of the plates on the order of hundreds of microns can help to avoid this problem by lowering the stiffness of the implant material.^{20,22} Internal porosity or functional channels can also be placed for the passage of materials, either synthetic polymer textiles during surgery or biological tissues and fluids after surgery. The flexibility of the 3D printing process means that it is possible to design a device to meet specific functional needs with minimized geometric constraints, rather than to satisfy the geometric constraints of the manufacturing process.^{17,19}

Ti alloy (Ti-6Al-4V) is one of the most popular material choices for 3D printing medical implants. First developed for the aerospace industry, Ti-6Al-4V has a long history of clinical use due to its corrosion resistance, biocompatibility, and excellent mechanical properties.²³ Ti-6Al-4V is used in many orthopaedic devices, such as intramedullary nails, bone plates, bone screws, spinal fusion cages, and artificial joints. Selective laser melting (SLM) is one of several techniques available to 3D print Ti parts and was adopted to fabricate the FastForward bunion plate. SLM involves melting metal powder in a protective nonoxidizing atmosphere (usually argon) with a high intensity computer-controlled laser beam (generally ytterbium) that traces the quasi 2D geometry of desired parts in each layer.^{17,19,21,24} After exposure of a layer, a build chamber lowers slightly, fresh powder is spread above, and then the next layer is melted onto the lower layer, until the full-thickness part is produced.²⁰ SLM-produced parts are being used in the aerospace, automotive, electronic, chemical, and biomedical fields.¹⁸ Furthermore, SLM-fabricated plate properties can be tailored for specific applications by adjusting fabrication variables such as powder layer thickness, powder particle size, laser scan spacing or hatch distance, laser power, laser speed, and beam compensation.^{14,19}

Electron beam melting (EBM) is another 3D printing technique that uses a controlled electron beam, instead of a laser, to melt the metal powder. Although EBM has been a more widely used method for manufacturing orthopaedic devices, SLM offers several advantages over EBM. EBM uses a larger powder particle size and greater powder layer thickness than SLM, which results in a more pronounced stair step effect and a rougher rippled surface than SLM parts.^{25,26} The roughness of EBM parts can be twice that of SLM parts as the layer thickness is nearly twice the height.²⁷ Surface roughness plays a critical role in crack initiation since cracks will start at surface defects like pores, crevices, and voids. Because SLM parts have a smoother surface, the base metal exhibits a higher tensile strength, yield strength, and fatigue strength for as-built SLM parts compared with EBM parts. Another 3D printing method similar to SLM is selective laser sintering (SLS). Whereas SLM completely melts the metal powder, SLS only partially melts the surface of metal particles to join them in a more or less porous structure, producing parts with rough surfaces, voids, and cracks. Unlike SLS, SLM can fabricate parts with less cracks and voids allowing the material properties to be retained close to those of the original bulk materials. In particular, porous SLM-fabricated Ti specimens have been shown to display higher compressive strength than the same structures composed by powder sintering²⁰ and even superior hardness and compressive and tensile strengths compared with similar parts formed through traditional casting and machining methods.^{15,17}

Mechanical Testing of 3D Printed Ti-6Al-4V

The fatigue strength of any orthopaedic implant is critical to ensure long-term clinical success. This is particularly the case with foot and ankle plates as these implants are subjected to repetitive loading under weight-bearing activities. The mechanical properties, including fatigue strength, of an implant material can vary widely depending upon the 3D printing technique and fabrication parameters used. Under certain conditions, these changes can negatively impact the mechanical performance of the implant itself resulting in breakage or instability. For example, surface defects/cracks created through the 3D printing process or sharp edges inherent in the implant design can reduce the fatigue strength potentially leading to

implant failure. Despite having fewer pores or voids compared with cast parts,¹⁵ SLM-produced parts, particularly thin plates, can still exhibit an external roughness that is susceptible to forming cracks and defects.

Various postmanufacturing processes have been suggested to improve the surface finish and reduce any edge effects of 3D printed parts and were consequently considered with the fabrication of the FastForward plate. In particular, the mechanical properties of SLM Ti-6Al-4V alloy after undergoing several postprocessing methods were evaluated. For the testing, dogbone-shaped specimens were manufactured by SLM. One sample group underwent a polishing process while a second sample group was left unpolished. Both groups were subsequently anodized according to SAE AMS 2488D. Samples (n=3/group) were tested under tension to failure at a displacement rate of 1 mm/min using a MTS Satec 20 kip servo-controlled, hydraulically actuated test frame. The monotonic tensile properties are given in Table 1 for the unpolished and polished samples, along with the properties of cast Ti-6Al-4V for comparison. The tensile properties of cast Ti-6Al-4V, obtained from the literature, are listed as this is a common manufacturing method for orthopaedic implants.²⁸ The yield strength and ultimate strength of all 3 are comparable; however, the polished SLM samples exhibit higher elongation capacity and consequently provide higher toughness relative to the unpolished SLM samples.

Fatigue tests were subsequently performed at increasingly lower stress levels below the yield strength of the samples to generate Stress-Cycle Life (S-N) curves and determine the fatigue strength for each material (Fig. 2). Fatigue tests were run on the same MTS Satec frame in axial stress control at a frequency of 5 Hz with R=0.1 (n ≥ 2/stress level). Tests were run until failure or run-out, which was defined as >2,000,000 cycles. A fatigue life curve of cast Ti-6Al-4V is provided as a comparison.²⁸ The fatigue strength was 200 MPa for the unpolished SLM samples, 450 MPa for the polished SLM samples, and 464 MPa for the cast samples. The unpolished samples exhibited lower fatigue strength than the polished and cast samples due to their rough surface, which is well known to create multiple sites for fatigue crack initiation. This fatigue strength is in agreement with the fatigue strength of other unpolished SLM samples, 200 to 230 MPa.^{29–32} The fatigue strength of the polished SLM samples was comparable with the cast Ti-6Al-4V potentially due to the decreased the number of sites for crack initiation from the polishing. Other studies of polished SLM samples have reported comparable fatigue strengths ranging from 350 to 620 MPa.^{29–33} These results indicate that the postprocessing polishing provides the SLM Ti alloy with superior mechanical performance and could potentially aid in reducing the likelihood of implant mechanical failure. On the basis of these results, these postmanufacturing processes were used on the FastForward plate.

TABLE 1. Monotonic Tensile Properties of 3D Printed (SLM) Ti-6Al-4V

Fabrication Method	Yield Strength (MPa)	Ultimate Tensile Strength (MPa)	Elongation (%)
SLM	897 ± 2	937 ± 1	16 ± 2
SLM + Polish	883 ± 17	946 ± 16	21 ± 1
Cast	877 ± 9	916 ± 7	9.4 ± 1.5

SLM indicates Selective laser melting; 3D, three-dimensional.

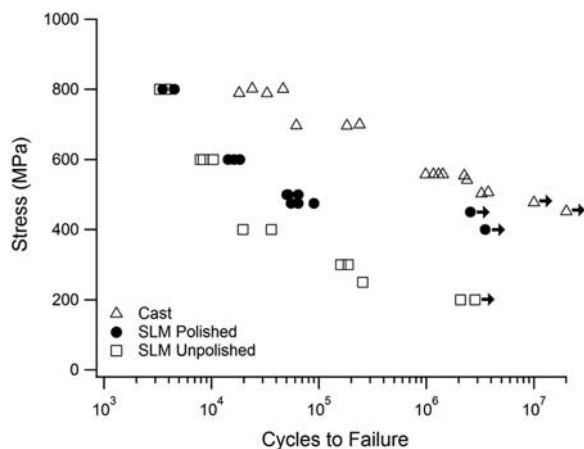


FIGURE 2. Fatigue life curve of cast, polished selective laser melting (SLM), and unpolished SLM Ti-6Al-4V extra low interstitial. Black arrow denotes tests that were stopped due to run-out.

FASTFORWARD TETHERING PROCEDURE

Current Tethering Approaches: Issues and Limitations

Metatarsus primus adductus (varus) development with clinical subluxation of the first MTP joint is a progressive course, and as the degree of metatarsus adductus increases, the development of hallux valgus can become more accelerated. First ray hypermobility is also a contributing factor in the development of flexible metatarsus primus adductus. Whereas normal first ray motion in the sagittal plane is approximately 5 mm dorsal and 5 mm plantar, the range of motion with hypermobile first rays is much higher resulting in forefoot supinatus upon full weight-bearing, higher medial column loading, and consequently an increase in transverse splaying force.

Most corrective surgical procedures involve osteotomizing the first metatarsal or fusing its adjacent joints to realign the first ray. However, these procedures have their own trade-offs with regards to the amount of correction that can be provided and length of postoperative recovery. For example, a head, or distal, osteotomy can only correct mild deformities since the metatarsal head can only be moved over a limited amount to maintain the desired 60% bone-to-bone contact between the capital fragment and the metatarsal. Although a proximal metatarsal osteotomy provides better IMA reduction compared with a distal osteotomy, this procedure is associated with complications such as, nonunion, malunion, recurrence, and avascular necrosis and first metatarsal shortening.^{34–39} Some proximal osteotomies also require the patient to be either non-weight-bearing or in a boot or sandal for 6 weeks.

Tethering of the first and second metatarsal is an alternative approach that reduces the first-second IMA while sparing the first metatarsal bone. The concept of tethering was first introduced almost a century ago with suture material or screws being used as the tethering apparatus.^{40–42} Today, a variety of devices, mostly suture buttons, are available. Unlike many osteotomy and Lapidus fusion procedures that require longer recovery to allow for bone healing, tethering approaches allow patients to weight-bear sooner, within 1 to 2 weeks.^{4,6} Although less obvious, tethering procedures can also control the hypermobility of the first ray in both the sagittal

and transverse planes by having the “pseudoligament” created with the suture material between the first and second metatarsals restrict the first metatarsal dorsiflexion and splaying in the transverse plane. Although successful long-term outcomes have been reported,^{6,43} current tethering procedures are not without their own challenges, mostly related to the stresses placed on the second metatarsal by the tether itself.⁵ For example, a suture button construct requires a drill hole through the second metatarsal, which can become a stress concentrator. A lasso technique can be quite effective in reducing the IMA, until the suture lasso begins to cut or wear through the second metatarsal. Therefore, a modified tethering technique which utilizes a device that shields the second metatarsal from friction and tensile forces of the suture could potentially offer the ideal solution for reducing the IMA and correcting hallux valgus deformities.

FastForward Plate Design Rationale

By leveraging the advantages of the SLM 3D printing process, a metal bone plate (FastForward Bone Tether Plate; MedShape Inc.) has been developed to aid in surgically reducing the first/second IMA in bunion correction surgeries without creating stress concentrations on the second metatarsal. The implant rests against the second metatarsal lateral cortex and serves to retain suture tape around the bone. Ti-6Al-4V ELI grade 23 powder was selected as the 3D printing material to provide the Ti alloy with improved ductility and better fracture toughness over non-ELI powder. After SLM fabrication, the plate is then subjected to postprocessing surface treatment to maintain the appropriate strength and fatigue properties as highlighted in Table 1 and Figure 2.

By 3D printing the FastForward plate, several key features could be incorporated into the design without introducing high manufacturing costs (Fig. 3). The broad geometry of the plate body helps uniformly distribute the force applied from tensioned suture tape across the bone, while a pair of buttress wings, extending from the plate body, act to further secure the plate to the second metatarsal and shield the dorsal and plantar cortices from tape friction. The dorsal wing is also slightly longer than the plantar wing mirroring the asymmetric dorsal-plantar geometry of the second metatarsal. A low-profile channel on the top of the plate body keeps the suture tape centered on the plate and over the buttress wings. This feature is important as the suture tape would be unable to hold the

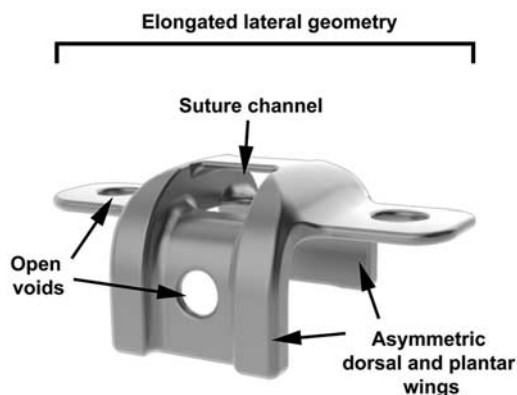


FIGURE 3. Illustration of three-dimensional printed Ti-6Al-4V extra low interstitial plate showing the features that were incorporated into the design by using three-dimensional printing techniques.

plate in place if not centrally oriented over the plate. Without 3D printing, this internal channel would be extremely difficult and costly to manufacture.

Furthermore, several open voids, added to the wings, reduce the plate-to-bone contact ratio and facilitate tissue ingrowth around and within the implant as a means to provide long-term stability.²⁴ Without this internal channel and open voids, the plate might need to be screwed to the bone for stability. Such holes in the second metatarsal are the root cause of failure of other bone-sparing correction approaches. Lastly, the plate has an overall thin profile, with a thickness similar to other low profile forefoot plating systems, to prevent it from protruding and causing any skin irritation. The slightly more prominent suture channel is also designed to rest on the lateral aspect of the second metatarsal where there is more surrounding soft tissue. Using traditional manufacturing methods, such a small, thin implant with complex features would be costly to produce, threatening its economic viability. Instead, the SLM 3D printing process reduces the manufacturing costs while not having to compromise on the features included into the design.

The 3D printed plate is part of the FastForward Bunion Correction System, a new tethering approach that addresses the issues with current tethering approaches that use suture cerclage or suture button devices. The approach broadly involves (1) wrapping suture tape around the plate and second metatarsal and securing it in a cow hitch knot, (2) reducing the first intermetatarsal space and then (3) fixing the tape in the first metatarsal with two interference screws. By reducing the actual IMA via a “pseudo-ligament,” the amount of IMA reduction is not limited. However unlike other tethering procedures (ie, suture button devices), no drill hole is placed in the more vulnerable second metatarsal, since, as described in the next section, such drilling can create an unwanted stress concentration.⁵

Biomechanical Testing

Biomechanical testing has been performed to evaluate the utility of the FastForward plate in preserving the mechanical integrity of the second metatarsal in comparison with the Mini-TightRope suture button (Arthrex, Inc., Naples, FL), another joint sparing corrective device. A novel benchtop model was developed to recreate the bending loading scenario imparted on the second metatarsal by the correction procedure. Simulated second metatarsals were fabricated out of 20PCF polyurethane foam block (Pacific Research Laboratories, Vashon, WA) with an elliptical cross section, and each suture fixation device was applied to the second metatarsal per the recommended technique. The FastForward plate was placed on the second metatarsal with the suture tape tied in a cow hitch knot around the bone (Fig. 4). For the Mini-TightRope, a 1.1-mm hole was drilled through the bone and the suture fed through the drill hole with the button device resting on the bone material. To determine the role of the plate in distributing forces in the cow hitch knot method, testing was also performed on the suture tape in a cow hitch knot without the plate. The suture or suture tape was pulled in tension in a transverse direction to the long axis of the approximated second metatarsal to simulate the tension applied by the IMA reduction. The maximum force required to break the second metatarsal under this bending scenario was measured (n=5). Results showed that the cow hitch knot approach alone produced higher failure loads than the Mini-TightRope (Fig. 5). The highest failure load was achieved when the FastForward plate was applied with the cow hitch knot, almost 3 times higher

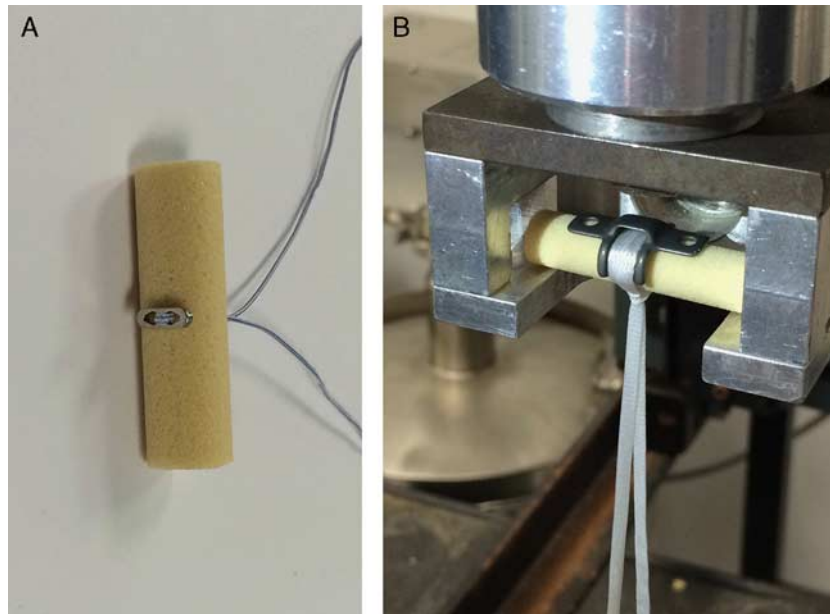


FIGURE 4. Images of Mini-TightRope affixed in “second metatarsal” synthetic bone (A) and three-dimensional printed plate and suture tape wrapped around second metatarsal, per the FastForward procedure, and loaded in the mechanical testing setup (B). full color online

than the fracture load with the Mini-Tightrope. These results suggest that the plate offers better fracture resistance of the second metatarsal when used to reduce the first-second IMA in bunion corrective surgery.

Surgical Technique

The FastForward plate and its associated components are applied in a relatively simple procedure. In some instances, adjunctive procedures may be required to correct an abnormal distal metatarsal angle, abducted or pronated hallux, or an abnormally long first metatarsal. These can be addressed with an appropriate head osteotomy for metatarsal shortening/decompression or, if necessary, de-rotation with a head (Reverdin type) osteotomy during the same surgical setting without interfering with the FastForward apparatus. If the

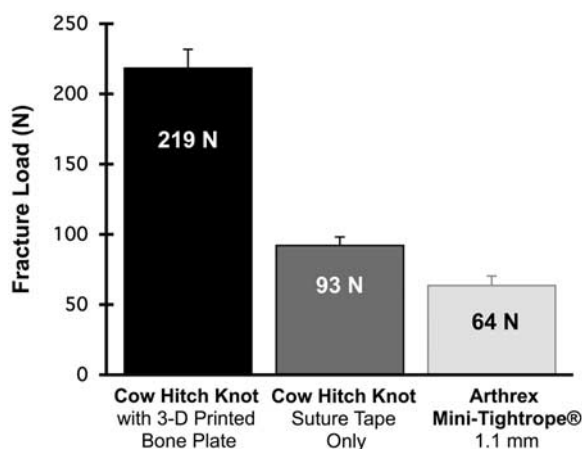


FIGURE 5. Biomechanical comparison of the three-dimensional (3D) printed plate with suture tape (the FastForward procedure), suture tape tied in knot, and the Mini-TightRope. Values represent the average (\pm SD) load required to break the second metatarsal.

hallux has its own deformity (hallux interphalangeus), this can also be addressed separately with an osteotomy of the phalanx.

The patient is placed supine on a radiolucent operating room table, and a proximal thigh tourniquet is utilized. A medial longitudinal incision is made from the hallux MTP joint to the midshaft of the first metatarsal. The dorsomedial cutaneous nerve branch of the superficial peroneal nerve is mobilized and retracted dorsally. A medial longitudinal capsulotomy is performed, and full-thickness capsular flaps are developed dorsally and plantarly to expose the medial eminence and MTP joint. A distal soft tissue release is performed through an intra-articular approach with pie crusting of the lateral joint capsule, release of the adductor hallucis (to address pronation if necessary), and release of the lateral sesamoid suspensory complex. The hallux is then stressed in varus to confirm adequate release. If the distal portion of the medial eminence blocks varus manipulation of the proximal phalanx, then partial resection of the distal bunion is recommended at this time. Complete medial eminence resection is not recommended at this stage in patients with poor bone stock as this may result in fracture or bone impaction at the first metatarsal head/neck junction.

A second dorsal longitudinal incision measuring approximately 2.5 to 3 cm is made over the second metatarsal shaft just proximal to the neck. Extensor tendons to the second toe are retracted laterally, and subperiosteal dissection is performed along the second metatarsal shaft both medially and laterally. A trial sizer is placed along the lateral aspect of the second metatarsal shaft to determine the appropriate plate size (small, medium, or large). A suture retriever guide is passed subperiosteally beneath the second metatarsal taking care not to trap the flexor tendon. A nickel Ti (NiTiNOL) suture lasso is then fed from lateral to medial through the retriever guide until the loop emerges on the medial side. Suture tape is passed through the lasso loop until there is equal length of suture tape on either side of the lasso. The lasso is then pulled on the lateral side through the retriever guide until the loop end of the suture tape emerges on the lateral side of the second metatarsal

(Fig. 6A). After removing the retriever guide, the suture tape is passed using the lasso through the suture channel on the appropriately sized plate (Fig. 6B). The plate is then placed on the lateral side of the second metatarsal ensuring the wing with a hole is on the dorsal side. A cow hitch knot is then created by passing the free ends of the suture tape through the looped portion. The plate is laid flat along the lateral second metatarsal shaft with the cow hitch knot adjusted to rest on the medial side of the bone (Fig. 6C).

Next, a guidewire is advanced under fluoroscopic guidance from medial to lateral across the first metatarsal directly adjacent to the center of the plate, angling this slightly from plantar-medial to dorsolateral to accommodate for any first metatarsal pronation and facilitate suture tape retrieval through the dorsal incision. Then, blunt dissection is carried out approximately 1.5 cm proximal to the first drill hole along the medial aspect of the first metatarsal diaphysis. A second guidewire is placed from medial to lateral directed slightly dorsally toward the second metatarsal incision. Both holes are then over-drilled with a 4.0-mm cannulated drill bit and 4.75-mm tap.

The lasso is then used to retrieve the suture tape through the distal hole from lateral to medial, beneath the muscle, and out the medial side of the first metatarsal (Fig. 6D). Continuing to use the lasso, the suture tape is then passed beneath any subcutaneous tissues along the medial first metatarsal shaft, and through the proximal drill hole out the lateral side where it can be retrieved from the dorsal incision. A hemostat is clamped on the free ends of the suture tape to prevent inadvertent migration out of the proximal hole.

Next, reduction of the first/second IMA is performed and confirmed under fluoroscopy. A 4.75-mm PEEK interference screw is inserted bicortically into the distal hole to fixate the tape. A screw depth gauge can be inserted in each drill hole to determine the appropriate screw length. With the suture tape tensioned in the distal direction, the screw is placed adjacent to the suture tape along its proximal aspect until it is flush with the bone on the medial side (Fig. 6E). Reduction should be confirmed fluoroscopically at this point before proceeding to ensure that the IMA is maintained. Although tensioning the suture tape in the lateral direction through the dorsal incision, a second bicortical 4.75-mm PEEK interference screw is secured adjacent to the suture tape in the proximal hole. Redundant suture tape can be excised and tucked into the intermetatarsal space. Completion of the medial eminence resection can be performed per surgeon preference and the procedure completed by imbricating the medial capsule and closing the incisions. A bunion strapping is applied.

Postoperatively, the patient is allowed to weight-bear as tolerated on the operative extremity in a Darco Ortho-Wedge sandal or Cam Walker boot. Non-weight-bearing x-rays of the foot are obtained at the first postoperative appointment and weight-bearing x-rays of the foot are obtained 4 to 6 weeks after surgery. Weekly restrapping of the hallux is performed during the first 4 to 6 weeks. In less complex cases, the patient may transition into comfortable wide toe box shoes 4 to 6 weeks after surgery and use a toe spacer for an additional 4 to 6 weeks.

Clinical Examples

To date, the clinical authors have performed over 60 cases total and have found the FastForward to be particularly advantageous in challenging, complex cases. For example, a juvenile bunion deformity is predicted to progress in severity at an accelerated rate. Bone altering osteotomies and joint fusions must be deferred until after skeletal maturity, when the deformity has often progressed further. The possible benefit of inserting a “pseudoligament” construct, such as the FastForward system that does not interfere with growth plates, to control the progression of hallux valgus is quite promising. Another challenging case is the recurrent bunion deformity with hypermobility. This type of case generally presents with the challenge of a narrow metatarsal head due to prior eminence removal. Although midshaft or proximal osteotomies may reduce first ray hypermobility using scar tissue,⁴⁴ FastForward’s tethering apparatus structurally limits first ray hypermobility and thereby reduces the splaying force while avoiding joint fusion or osteotomy. Here, 2 clinical examples are presented where FastForward was used to correct hallux valgus and metatarsus primus adductus.

Case Example 1

A 16-year-old healthy girl presented with bilateral congenital hallux valgus deformities that became symptomatic at age 14. She had a family history of bunion deformities on her maternal side. She reported that the bunion on the left had become progressively bigger and more painful over the previous year. She rated her bunion pain at 8/10, worse in closed shoes and with physical activity (cheerleading).

On examination, she had mild bursitis with pain to palpation over the medial eminence and demonstrated a moderate hallux valgus deformity with metatarsus primus varus, which was manually reducible. First MTP joint range of motion was normal. Evaluation of the first ray revealed hypermobility in both the sagittal and transverse planes. First ray hypermobility



FIGURE 6. Surgical photos showing the key steps in the FastForward procedure: suture tape is passed underneath the second metatarsal (A), the tape is fed through the channel on the three-dimensional printed plate (B), the plate is placed on the lateral side of the second metatarsal and the tape is looped into a cow hitch knot (C), after drilling 2 holes in the first metatarsal, the tape is passed across the first-second intermetatarsal space using a suture lasso (D), and 2 screws are inserted to fixate the tape inside the first metatarsal (E).

in the sagittal plane was noted with 15 mm dorsal and 10 mm plantar motion (25 mm total) of the first metatarsal relative to the second metatarsal (normal 10 mm total). Hypermobility in the transverse plane was also noted as the intermetatarsal space was clinically reducible by manually pushing the first metatarsal head laterally while distracting the hallux, deeming this a reducible metatarsus primus varus deformity and an ideal case for a tethering procedure such as FastForward, as opposed to an osteotomy or joint fusion. Initial radiographic evaluation demonstrated a hallux valgus angle (HVA) of 30.3 degrees and an IMA of 16 degrees (Fig. 7A). There was subluxation of the sesamoid apparatus with three fourths of the fibular sesamoid visible in the first-second intermetatarsal space.

The patient elected to proceed with left bunion correction, as this was the more symptomatic foot. The hallux valgus and metatarsus primus varus deformities were corrected using the FastForward procedure as described in Section D. She was allowed to partially weight-bear as tolerated in a CAM Walker boot. One week postoperatively, partial weight-bearing x-rays showed a HVA of 0 degrees and IMA of 1.0 degrees. She reported only mild pain during the first week, but did report a feeling of tightness inside the foot initially. At her 6 week postoperative appointment, she denied any pain and weight-bearing x-rays demonstrated HVA of 0 degrees and IMA of 3.8 degrees. She then transitioned to regular shoes and resumed normal activity to tolerance. At 12 weeks postoperatively, she was active and pain free and the feeling of “tightness” had fully resolved. Her x-rays showed HVA of 0 degrees and IMA of 5.0 degrees. At her 11 month postoperative visit her x-rays demonstrated that her reduction was maintained with HVA of 0 degrees and IMA of 5.0 degrees (Fig. 7B). Clinically her first ray hypermobility had been reduced to normal (10 mm total sagittal plane motion of the first metatarsal relative to the second metatarsal). First MTP joint range of motion was also

normal. The patient on her own reported that the left foot appeared to have more of an arch and also that her left foot felt more stable than her right foot. Clinically, this could be explained by the reduction of first ray hypermobility. The patient was pain free on her left foot and wished to pursue correction of her right bunion deformity using the FastForward procedure.

Case Example 2

A 64-year-old woman with rheumatoid arthritis, osteoporosis, and hepatitis C presented with a painful left hallux valgus deformity, multiple large rheumatoid foot nodules, and a painful bunionette deformity. She recently recovered from rheumatoid nodule excision on her right foot and wished to move ahead with left foot surgical reconstruction. On examination, she demonstrated prominent, mobile, multilobulated rheumatoid nodules along the medial forefoot surrounding the hallux MTP joint as well as the lateral forefoot over the fifth MTP joint. The medial eminence was tender to palpation and moderate hallux valgus with mild pronation deformity was passively correctable to neutral. There was mild first ray hypermobility in addition to fourth and fifth toe overlap. Radiographic evaluation demonstrated HVA of 34 degrees, IMA of 13 degrees, and fifth MTP medial dislocation (Fig. 8A). She underwent rheumatoid nodule excision, the FastForward procedure and bunionette correction with a distal fifth metatarsal osteotomy. She was allowed to weight-bear as tolerated in a Darco Ortho-Wedge sandal. One week following surgery, non-weight-bearing x-rays showed improved HVA of 0 degrees and IMA 4.0 degrees. She complained of 5/10 pain and still required narcotic pain medication. Five weeks following surgery, she denied any foot pain and had discontinued all pain medications. At 12 weeks postsurgery, the patient was pleased with her results, continued to be pain free, and had



FIGURE 7. Preoperative (A) and 11-month postoperative (B) anteroposterior radiographs of a 16-year-old girl who underwent the FastForward procedure for a moderate congenital hallux valgus deformity.



FIGURE 8. Preoperative (A) and 12-week postoperative (B) weight-bearing anteroposterior radiographs of a 64-year-old woman with rheumatoid arthritis who underwent the FastForward procedure for a moderate hallux valgus deformity in addition to fifth metatarsal osteotomy for severe bunionette deformity.

transitioned to regular shoes. No hypermobility was noted, and weight-bearing x-rays at this time point showed HVA of 12 degrees and an IMA of 6.0 degrees (Fig. 8B).

CONCLUSIONS

Preliminary clinical results suggest that the FastForward procedure using the 3D printed bone tether plate is able to successfully correct hallux valgus deformities and allow patients to return to weight-bearing activities sooner at short-term and intermediate-term follow-up. The SLM 3D printing in combination with other postprocessing surface treatments provides the plate with comparable, and in some instances superior, fatigue strength compared with traditional plate manufacturing methods. The plate's unique design features aid in preserving the structural integrity of the second metatarsal both in the short-term by reducing stress concentrations and in the long-term by supporting tissue ingrowth. Future studies will focus on evaluating long-term clinical outcomes to determine the plate and FastForward system's efficacy and stability.

REFERENCES

1. Easley ME, Trnka HJ. Current concepts review: hallux valgus part I: pathomechanics, clinical assessment, and nonoperative management. *Foot Ankle Int.* 2007;28:654–659.
2. Canale ST. *Disorders of the Hallux Campbell's Operative Orthopaedics*, 12th ed. St. Louis, MO: Mosby; 2010:380–3901.
3. Easley ME, Trnka HJ. Current concepts review: hallux valgus part II: operative treatment. *Foot Ankle Int.* 2007;28:748–758.
4. Holmes GB Jr, Hsu AR. Correction of intermetatarsal angle in hallux valgus using small suture button device. *Foot Ankle Int.* 2013;34:543–549.
5. Weatherall JM, Chapman CB, Shapiro SL. Postoperative second metatarsal fractures associated with suture-button implant in hallux valgus surgery. *Foot Ankle Int.* 2013;34:104–110.
6. Wu DY. A retrospective study of 63 hallux valgus corrections using the osteodesis procedure. *J Foot Ankle Surg.* 2015;54:406–411.
7. Kluesner AJ, Morris JB. Opening wedge and anatomic-specific plates in foot and ankle applications. *Clin Podiatr Med Surg.* 2011;28:687–710.
8. Jastifer JR. Topical review: locking plate technology in foot and ankle surgery. *Foot Ankle Int.* 2014;35:512–518.
9. Ahmad M, Nanda R, Bajwa AS, et al. Biomechanical testing of the locking compression plate: when does the distance between bone and implant significantly reduce construct stability? *Injury.* 2007;38:358–364.
10. Fulkerson E, Egol KA, Kubiak EN, et al. Fixation of diaphyseal fractures with a segmental defect: a biomechanical comparison of locked and conventional plating techniques. *J Trauma.* 2006;60:830–835.
11. Miller DL, Goswami T. A review of locking compression plate biomechanics and their advantages as internal fixators in fracture healing. *Clin Biomech (Bristol, Avon).* 2007;22:1049–1062.
12. Stoffel K, Dieter U, Stachowiak G, et al. Biomechanical testing of the LCP—how can stability in locked internal fixators be controlled? *Injury.* 2003;34(suppl 2):B11–B19.
13. Jayanthi P. 3D modeling, custom implants and its future perspectives in craniofacial surgery. *Ann Maxillofac Surg.* 2014;4:9–18.
14. Chen J, Zhang Z, Chen X, et al. Design and manufacture of customized dental implants by using reverse engineering and selective laser melting technology. *J Prosthet Dent.* 2014;112:1088–1095.
15. Kanazawa M, Iwaki M, Minakuchi S, et al. Fabrication of titanium alloy frameworks for complete dentures by selective laser melting. *J Prosthet Dent.* 2014;112:1441–1447.

16. Telfer S, Pallari J, Munguia J, et al. Embracing additive manufacture: implications for foot and ankle orthosis design. *BMC Musculoskeletal Disord.* 2012;13:84.
17. Attar H, Calin M, Zhang LC, et al. Manufacture by selective laser melting and mechanical behavior of commercially pure titanium. *Mater Sc Eng A.* 2014;593:170–177.
18. Yadroitsev I, Krakhmalev P, Yadroitsava I. Selective laser melting of Ti6Al4V alloy for biomedical applications: temperature monitoring and microstructural evolution. *J Alloys Compd.* 2014;583:404–409.
19. Challis VJ, Xu X, Zhang LC, et al. High specific strength and stiffness structures produced using selective laser melting. *Mater Des.* 2014;63:783–788.
20. Pattanayak DK, Fukuda A, Matsushita T, et al. Bioactive Ti metal analogous to human cancellous bone: fabrication by selective laser melting and chemical treatments. *Acta Biomater.* 2011;7:1398–1406.
21. Xiao D, Yang Y, Su X, et al. An integrated approach of topology optimized design and selective laser melting process for titanium implants materials. *Biomed Mater Eng.* 2013;23:433–445.
22. Van der Stok J, Van der Jagt OP, Amin Yavari S, et al. Selective laser melting-produced porous titanium scaffolds regenerate bone in critical size cortical bone defects. *J Orthop Res.* 2013;31:792–799.
23. Geetha M, Singh AK, Asokamani R, et al. Ti based biomaterials, the ultimate choice for orthopaedic implants—a review. *Prog Mater Sci.* 2009;54:397–425.
24. Fukuda A, Takemoto M, Saito T, et al. Osteoinduction of porous Ti implants with a channel structure fabricated by selective laser melting. *Acta Biomater.* 2011;7:2327–2336.
25. Koike MGP, Owen K, Lilly G, et al. Evaluation of titanium alloys fabricated using rapid prototyping technologies—electron beam melting and laser beam melting. *Materials.* 2011;4:1776–1792.
26. Rafi HK, Karthik NV, Gong H, et al. Microstructures and mechanical properties of Ti6Al4V parts fabricated by selective laser melting and electron beam melting. *J Mater Eng Perform.* 2013;22:3872–3883.
27. Chan K, Koike MMRL, Okabe T. Fatigue life of titanium alloys fabricated by additive layer manufacturing techniques for dental implants. *Metallurg Mater Trans A.* 2013;44A:1010–1022.
28. Oh J, Lee JG, Kim NJ, et al. Effect of thickness on fatigue properties of investment cast Ti-6Al-4V alloy plates. *J Mater Sci.* 2004;39:587–591.
29. Kasperovich G, Hausmann J. Improvement of fatigue resistance and ductility of TiAl6V4 processed by selective laser melting. *J Mater Process Technol.* 2015;220:202–214.
30. Rekedal K, Liu D. Fatigue life of selective laser melted and hot isostatically pressed Ti-6Al-4v absent of surface machining. *AIAA.* Kissimmee, FL; 2015.
31. Wycisk E, Emmelmann C, Siddique S, et al. High cycle fatigue (HCF) performance of Ti-6Al-4V alloy processed by selective laser melting. *Adv Mater Res.* 2013;816-817:134–139.
32. Wycisk E, Solbach A, Siddique S, et al. Effects of defects in laser additive manufactured Ti-6Al-4V on fatigue properties. *Phys Procedia.* 2014;56:371–378.
33. Leuders S, Thöne M, Riemer A, et al. On the mechanical behaviour of titanium alloy TiAl6V4 manufactured by selective laser melting: fatigue resistance and crack growth performance. *Int J Fatigue.* 2013;48:300–307.
34. Toth K, Huszanyik I, Kellermann P, et al. The effect of first ray shortening in the development of metatarsalgia in the second through fourth rays after metatarsal osteotomy. *Foot Ankle Int.* 2007;28:61–63.
35. Easley ME, Darwish HH, Schreyack DW, et al. Hallux valgus: proximal first metatarsal osteotomies. In: Saxena A, ed. *International Advances in Foot and Ankle Surgery.* London: Springer London; 2012:11–25.
36. Klemola T, Leppilahti J, Kalinainen S, et al. First tarsometatarsal joint derotational arthrodesis—a new operative technique for flexible hallux valgus without touching the first metatarsophalangeal joint. *J Foot Ankle Surg.* 2014;53:22–28.
37. Coetzee JC. Scarf osteotomy for hallux valgus repair: the dark side. *Foot Ankle Int.* 2003;24:29–33.
38. Cottom JM, Vora AM. Fixation of larpus arthrodesis with a plantar interfragmentary screw and medial locking plate: a report of 88 cases. *J Foot Ankle Surg.* 2013;52:465–469.
39. Mallette JP, Glenn CL, Glod DJ. The incidence of nonunion after Larpus arthrodesis using staple fixation. *J Foot Ankle Surg.* 2014;53:303–306.
40. Friscia DA. Distal soft tissue correction for hallux valgus with proximal screw fixation of the first metatarsal. *Foot Ankle Clin.* 2000;5:581–589.
41. Kelikian H. *Hallux Valgus, Allied Deformities of the Forefoot and Metatarsalgia.* Philadelphia, PA: Saunders; 1965.
42. Dayton P, Sedberry S, Feilmeier M. Complications of metatarsal suture techniques for bunion correction: a systematic review of the literature. *J Foot Ankle Surg.* 2015;54:230–232.
43. Wu DY. Syndesmosis procedure: a non-osteotomy approach to metatarsus primus varus correction. *Foot Ankle Int.* 2007;28:1000–1006.
44. Coughlin MJ, Jones CP. Hallux valgus and first ray mobility. A prospective study. *J Bone Joint Surg Am.* 2007;89:1887–1898.